

Micromechanical Modeling of Reinforcement Fracture in Zirconium Carbide/4015 Particle-Reinforced Metal-Matrix Composites

¹V. V. Satyanarayana and A. Chennakesava Reddy²

¹Associate Professor, Department of Mechanical Engineering, Vasavi College of Engineering, Hyderabad, India

²Associate Professor, Department of Mechanical Engineering, Vasavi College of Engineering, Hyderabad, India
dr_acreddy@yahoo.com

Abstract: In the present work, the ZrC/AA4015 alloy metal matrix composites were subjected to mechanical and thermal loads. The results obtained from the finite element analysis and experimental procedure of ZrC/AA4015 alloy composites reveals the interphase separation from the particle and the matrix. Also, the particle fracture has been noticed in 30% ZrC/AA4015 composites above 250°C.

Keywords: Zirconium carbide, AA4015 alloy, RVE model, finite element analysis, interphase separation, particle fracture.

1. INTRODUCTION

The performance of particle reinforced composites is influenced by not only the component properties and component concentrations, but also the interfacial interaction between the particles and the matrix. In particular, the inclusion of stiff particles to a soft matrix can lead to an increase in composite stiffness, strength, impact resistance, and abrasion resistance. At large deformations, particles tend to debond from the matrix, influencing both the ductility and fracture toughness of the composite. To enhance or control these properties, the particles themselves can be tailored through surface treatments. The chemical between the particle and the matrix may result in the formation of an interphase between them during manufacturing and processing. Even though these interphases are typically microscopic, they can greatly influence the macroscopic behavior of composite materials. The extent and composition of this interphase depends on a number of factors, including the surface area and surface treatment of the particles, as well as the level of mixing and age of the composite. The numerical investigation of interfacial debonding using the cohesive element method was pioneered by Needleman [1]. There have been many traction–separation relations which have seen widespread use; including linear, bilinear, trapezoidal, polynomial, and exponential softening relations [2-15].

There are four primary factors which influence the macroscopic constitutive response of particle reinforced composites: component properties, component concentrations, type of loading, and interfacial debonding. This paper presents a computational framework capable of capturing the influence of volume fraction of zirconium carbide (ZrC) particles and thermo-mechanical loading on interphase separation and particle fracture. The shape zirconium carbide nanoparticle considered in this work is spherical. The periodic particle distribution was a square array and corresponding representative volume element (RVE) is showed in figure 1.

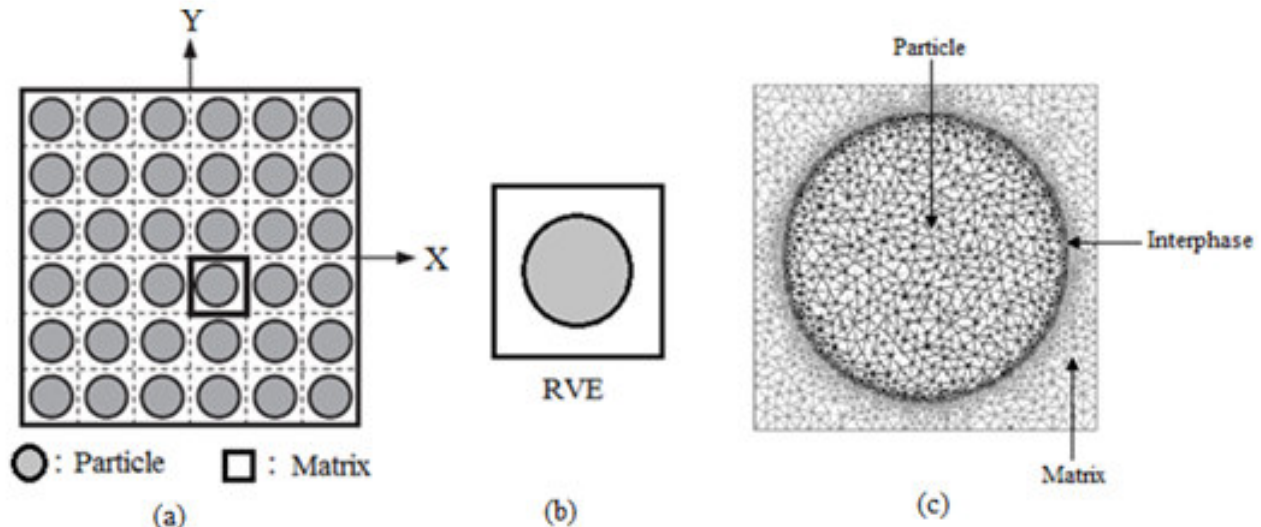


Figure 1: Square array of particles (a); Representative Volume Element (b); and Discretization of RVE (c).

2. MATERIALS METHODS

The matrix material was AA4015 alloy. The reinforcement material was zirconium carbide (ZrC) nanoparticles of average size 100nm. The mechanical properties of materials used in the present work are given in table 1. In the current work, a cubical representative volume element (RVE) was implemented to analyze the tensile behavior ZrC/AA4015 alloy composites at two (10% and 30%) volume fractions of ZrC and at different temperatures. The large strain PLANE183 element was used in the matrix in all the models. In order to model the adhesion between the matrix and the particle, a CONTACT 172 element was used.

Table 1: Mechanical properties of AA4015 matrix and ZrC nanoparticles

Property	AA4015	ZrC
Density, g/cc	2.71	6.73
Elastic modulus, GPa	68.9	430.0
Coefficient of thermal expansion, 10 ⁻⁶ 1/°C	18.0	6.8
Specific heat capacity, J/kg/°C	850	368
Thermal conductivity, W/m/°C	138	25
Poisson's ratio	0.33	0.25

3. RESULTS AND DISCUSSION

Figure 2 shows the variation of effective material properties such as Young's modulus, shear modulus and Poisson's ratio with the change in temperature of the composites. Figure 2a shows the variation of modulus in the loading direction, E_x, and in the transverse direction of loading, E_y, with the variation of the temperature. It is observed that when the temperature is increased from 30°C to 300°C, the normalized elastic modulus, E_x/E_m, is decrease; wherein E_m is the elastic modulus of the matrix. The similar trend is also observed for E_y/E_m. The normalized shear modulus increases with increase of temperature (figure 2b). The values of the major Poisson's ratio, ν_{xy}, are decreased with the increasing of temperature except at 100°C of temperature (figure 2c). The uneven distribution of Poisson's ratio for ν_{xy} is not clear.

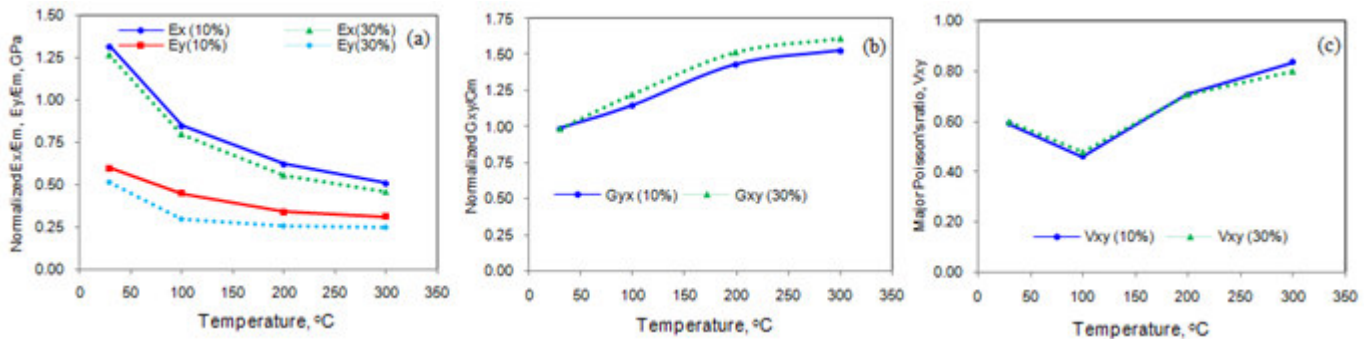


Figure 2: Effect of temperature on micromechanical properties of ZrC/AA4015 composites.

If the particle deforms in an elastic manner (according to Hooke's law) then,

$$\tau = \frac{n}{2} \sigma_p \tag{1}$$

where σ_p is the particle stress. For the interfacial debonding/yielding to occur, the interfacial shear stress reaches its shear strength:

$$\tau = \tau_{max} \tag{2}$$

For particle/matrix interfacial debonding can occur if the following condition is satisfied:

$$\tau_{max} < \frac{n\sigma_p}{2} \tag{3}$$

It is observed from figure 3a that the interphase separation occurs between ZrC nanoparticle and AA4015 alloy matrix as the condition in Eq.(3) is satisfied in 10% ZrC/AA4015 composites below 250°C while the interphase separation occurs below 100°C in 30% ZrC/AA4015 composites. The normal displacement field (figure 4) across the interphase increases with increase of temperature. This might be due to the fact of interphase separation between the particle and the matrix. Further, the normal and tangential tractions (figure 5) along the interphase increase with increase of temperature to take place the interphase separation from ZrC particle and AA4015 alloy matrix. Because of the mismatch in Poisson's ratio and Young's modulus, the matrix above and below the particle is confined and a state of expansion is developed above and below the particle. Due to flow of

matrix around the particle splitting force pulls the matrix away from the particle. Due to this splitting force, tensile zone is developed where maximum failure stress reaches the tensile strength of the matrix.

If particle fracture occurs when the stress in the particle reaches its ultimate tensile strength, $\sigma_{p,uts}$, then setting the boundary condition at

$$\sigma_p = \sigma_{p, uts} \tag{4}$$

The relationship between the strength of the particle and the interfacial shear stress is such that if

$$\sigma_{p, uts} < \frac{2\tau}{n} \tag{5}$$

Then the particle will fracture. From the figure 3b, it is observed that the ZrC nanoparticle was fractured above 200°C in 10% ZrC/AA4015 composites and above 100°C in 30% ZrC/AA4015 composites as the condition in Eq. (5) is satisfied. The von Mises stress as a function of temperature is illustrated in figure 6. Red zone in Figure 6 indicates the tensile zone where stress is higher and this tends to separate the interface from the particle and the matrix. The particle fracture was occurred due to thermal shock.

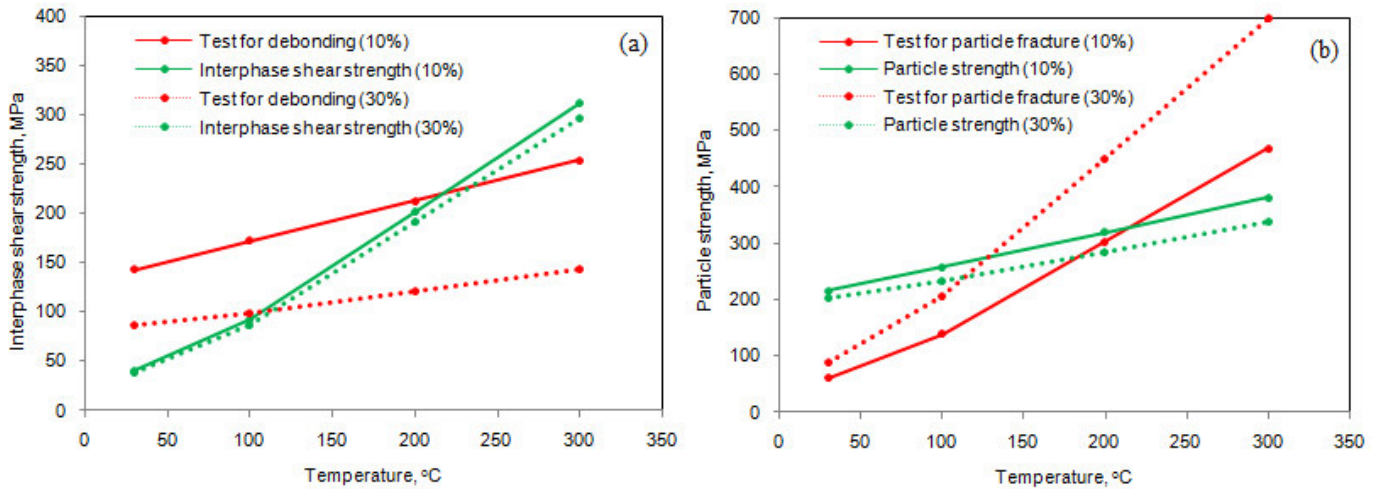


Figure 3: Criterion for interfacial debonding (a) and for particle fracture (b).

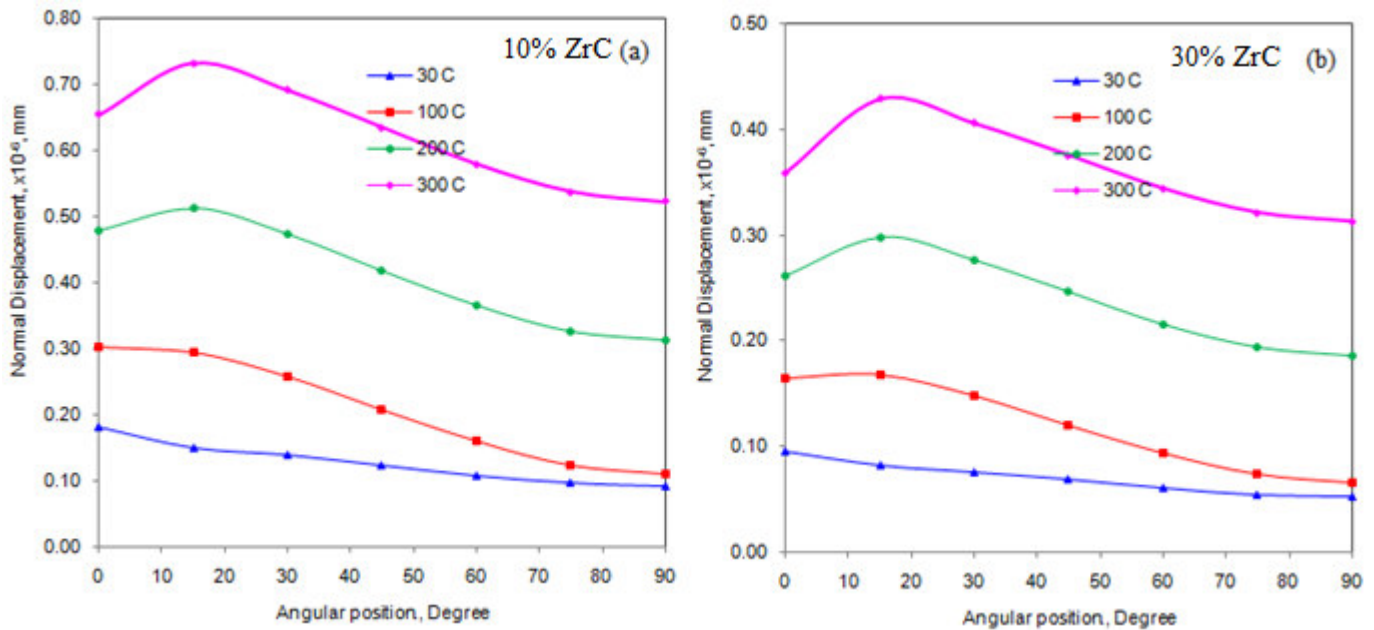


Figure 4: Normal displacement across the interphase between ZrC particle and AA4015 alloy matrix.

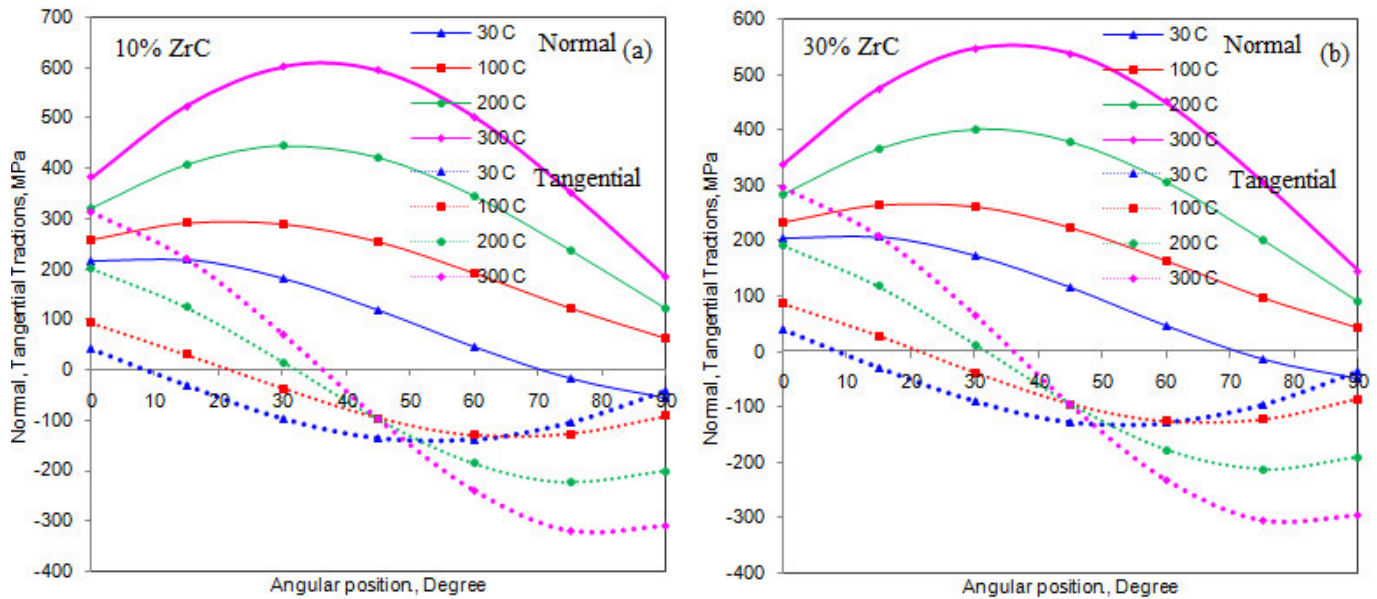


Figure 5: Normal and tangential tractions along the interphase.

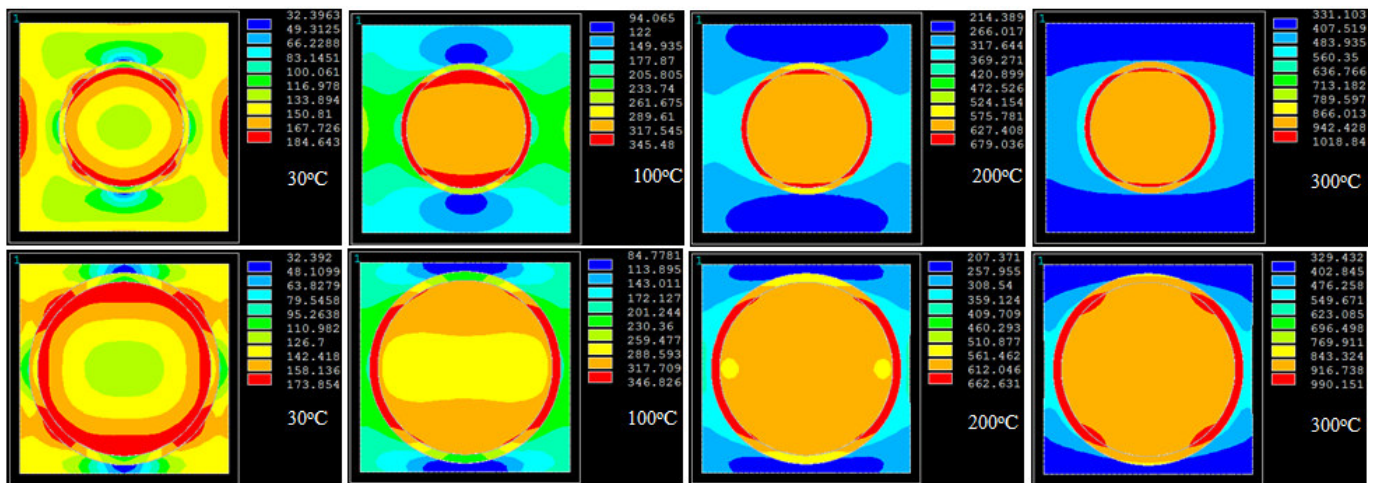


Figure 6: Images of von Mises stresses obtained from FEA: (a) 10% ZrC/AA4015 alloy and (b) 30% ZrC/AA4015 alloy composites.

4. CONCLUSION

The analysis could predict the decreasing trend of elastic moduli of the specimen and increasing trend of the shear modulus of the material with respect to increase of temperature. The interphase separation has occurred between the particle and the matrix. The particle fracture has also occurred in ZrC/AA4015 composites.

REFERENCES

1. A. Needleman, Continuum model for void nucleation by inclusion debonding, ASME Journal of Applied Mechanics, 54, 1987, pp. 525-531.
2. A. Chennakesava Reddy, Evaluation of Debonding and Dislocation Occurrences in Rhombus Silicon Nitride Particulate/AA4015 Alloy Metal Matrix Composites, 1st National Conference on Modern Materials and Manufacturing, Pune, India, 19-20 December 1997, pp. 278-282.
3. A. Chennakesava Reddy, Interfacial Debonding Analysis in Terms of Interfacial Tractions for Titanium Boride/AA3003 Alloy Metal Matrix Composites, 1st National Conference on Modern Materials and Manufacturing, Pune, 19-20 December, 1997.
4. A. Chennakesava Reddy, Assessment of Debonding and Particulate Fracture Occurrences in Circular Silicon Nitride Particulate/AA5050 Alloy Metal Matrix Composites, National Conference on Materials and Manufacturing Processes, Hyderabad, India, 27-28 February 1998, pp. 104-109.
5. A. Chennakesava Reddy, Local Stress Differential for Particulate Fracture in AA2024/Titanium Carbide Nanoparticulate Metal Matrix Composites, National Conference on Materials and Manufacturing Processes, Hyderabad, India, 27-28 February 1998, pp. 127-131.

6. A. Chennakesava Reddy, Micromechanical Modelling of Interfacial Debonding in AA1100/Graphite Nanoparticulate Reinforced Metal Matrix Composites, 2nd International Conference on Composite Materials and Characterization, Nagpur, India, 9-10 April 1999, pp. 249-253.
7. A. Chennakesava Reddy, Cohesive Zone Finite Element Analysis to Envisage Interface Debonding in AA7020/Titanium Oxide Nanoparticulate Metal Matrix Composites, 2nd International Conference on Composite Materials and Characterization, Nagpur, India, 9-10 April 1999, pp. 204-209.
8. H. B. Niranjana, A. Chennakesava Reddy, Computational Modeling of Interfacial Debonding in Fused Silica/AA7020 Alloy Particle-Reinforced Metal Matrix Composites, 3rd International Conference on Composite Materials and Characterization, Chennai, India, 11-12 May 2001, pp. 222-227.
9. H. B. Niranjana, A. Chennakesava Reddy, Nanoscale Characterization of Interfacial Debonding and Matrix Damage in Titanium Carbide/AA8090 Alloy Particle-Reinforced Metal Matrix Composites, 3rd International Conference on Composite Materials and Characterization, Chennai, India, 11-12 May 2001, pp. 228-233.
10. S. Sundara Rajan, A. Chennakesava Reddy, Assessment of Temperature Induced Fracture in Boron Nitride/AA1100 Alloy Particle-Reinforced Metal Matrix Composites, 3rd International Conference on Composite Materials and Characterization, Chennai, India, 11-12 May 2001, pp. 234-239.
11. S. Sundara Rajan, A. Chennakesava Reddy, Estimation of Fracture in Zirconia/AA2024 Alloy Particle-Reinforced Composites Subjected to Thermo-Mechanical Loading, 3rd International Conference on Composite Materials and Characterization, Chennai, India, 11-12 May 2001, pp. 240-245.
12. P. M. Jebaraj, A. Chennakesava Reddy, Finite Element Predictions for the Thermoelastic Properties and Interphase Fracture of Titanium Nitride /AA3003 Alloy Particle-Reinforced Composites, 3rd International Conference on Composite Materials and Characterization, Chennai, India, 11-12 May 2001, pp. 246-251.
13. P. M. Jebaraj, A. Chennakesava Reddy, Effect of Thermo-Mechanical Loading on Interphase and Particle Fractures of Titanium Oxide /AA4015 Alloy Particle-Reinforced Composites, 3rd International Conference on Composite Materials and Characterization, Chennai, India, 11-12 May 2001, pp. 252-256.
14. A. Chennakesava Reddy, Effect of CTE and Stiffness Mismatches on Interphase and Particle Fractures of Zirconium Carbide /AA5050 Alloy Particle-Reinforced Composites, 3rd International Conference on Composite Materials and Characterization, Chennai, India, 11-12 May 2001, pp. 257-262.
15. A. Chennakesava Reddy, Behavioral Characteristics of Graphite /AA6061 Alloy Particle-Reinforced Metal Matrix Composites, 3rd International Conference on Composite Materials and Characterization, Chennai, India, 11-12 May 2001, pp. 263-269.